

## Line of compressibility maxima in the phase diagram of supercooled water

Francesco Sciortino,<sup>1,2</sup> Peter H. Poole,<sup>1,3</sup> Ulrich Essmann,<sup>1,\*</sup> and H. E. Stanley<sup>1</sup>

<sup>1</sup>*Center for Polymer Studies and Physics Department, Boston University, Boston, Massachusetts 02215*

<sup>2</sup>*Dipartimento di Fisica and Istituto Nazionale per la Fisica della Materia, Università di Roma La Sapienza, Piazzale Aldo Moro 2, I-00185, Roma, Italy*

<sup>3</sup>*Department of Applied Mathematics, University of Western Ontario, London, Ontario, Canada N6A 5B7*

(Received 12 July 1996; revised manuscript received 8 October 1996)

We evaluate thermodynamic, structural, and transport properties from extensive molecular-dynamics computer simulations of the ST2 and TIP4P models of liquid water over a wide range of thermodynamic states. We find a line in the phase diagram along which the isothermal compressibility of the supercooled liquid is a maximum. We further observe that along this line the magnitude of the maximum increases with decreasing temperature. Extrapolation to temperatures below those we are able to simulate suggests that the compressibility diverges. In this case, the line of compressibility maxima develops into a critical point followed at lower temperature by a line of first-order phase transitions. The behavior of structural and transport properties of simulated water supports the possibility of a line of first-order phase transitions separating two liquid phases differing in density. We therefore examine the experimentally known properties of liquid and amorphous solid water to test if the equation of state of the liquid might exhibit a line of compressibility maxima, possibly connected to a critical point that is the terminus of a line of phase transitions. We find that the currently available experimental data are consistent with these possibilities. [S1063-651X(97)09501-9]

PACS number(s): 64.70.Ja, 64.30.+t, 64.60.My

### I. INTRODUCTION

Though water is a common liquid, it is not a simple liquid [1–5]. In particular, its thermodynamic properties display a number of anomalies. For example, the density of water passes through a maximum at a temperature  $T=4^\circ\text{C}$  at a pressure  $P=1\text{ atm}$  [3]. Also, the isothermal compressibility  $K_T$  and the isobaric specific heat  $C_P$  pass through minima and begin to rise dramatically as  $T$  decreases [6,7].

The glassy state of water also exhibits rich behavior. As found by Mishima and co-workers [8–10], amorphous ice exhibits “polyamorphism” [11–14]. That is, it is observed to exist in at least two quite distinct forms: a low-density amorphous (LDA) ice and a high-density amorphous (HDA) ice. In addition, LDA ice and HDA ice are observed to convert from one to the other via abrupt changes in density [10].

The stability limit conjecture [6,15–17] ascribes the anomalies of water to the presence of a reentrant liquid-gas spinodal in the supercooled region of the phase diagram. Recent computer simulation studies of the ST2 [18] and TIP4P [19] potentials have shown that the spinodal is not reentrant for these models of water [20]. Moreover, based on these simulations, it was proposed that the anomalies of water are related to the existence of a critical point in the deeply supercooled region [21]. It was further proposed that the observed polyamorphism of the amorphous ices is due to the extension into the glassy regime of a line of first-order liquid-liquid phase transitions connected to the critical point [22–24].

Evidence for the occurrence of a critical point in ST2 and

TIP4P water was based on the behavior of the equation of state (EOS) of the supercooled liquid [20,21]. As we will show in detail below, the feature of the EOS used to support the proposal of a critical point can be described in terms of a line of thermodynamic states along which  $K_T$  is a maximum. Recently, however, theoretical work [25] has shown that a line of  $K_T$  maxima must occur in any liquid that (i) exhibits a line of density maxima having a negative slope in the  $P$ - $T$  plane and (ii) does not exhibit a reentrant spinodal. ST2 and TIP4P water satisfy both of these conditions [20]. Hence a line of  $K_T$  maxima need not necessarily be interpreted as due to the occurrence of a critical point. Rather, the line of  $K_T$  maxima may be viewed as due only to the thermodynamic behavior occurring at higher  $T$ .

Hence there are two possible behaviors for a liquid in which there is a line of  $K_T$  maxima, shown in Fig. 1. Either the line develops into a critical point, and is replaced at lower  $T$  by a line of phase transitions, or  $K_T$  remains finite for all  $T$  along the line of  $K_T$  maxima.

A brief report of the simulation results upon which the proposal of a critical point is based has been presented in Ref. [21]. In this article we provide a detailed analysis of the thermodynamic data obtained from these simulations and also evaluate structural and dynamical properties related to the thermodynamic behavior found in the supercooled liquid. A detailed description of the molecular-dynamics simulations from which the present data are derived is provided in Ref. [20].

Specifically, in Sec. II we locate the line of  $K_T$  maxima and examine its properties to determine if the proposal of a critical point remains valid in light of the theoretical developments described above. In Sec. III we show how the behavior of the internal energy supports the occurrence of a line of  $K_T$  maxima and also elucidates the thermodynamic

\*Present address: Department of Chemistry, University of North Carolina, Chapel Hill, NC 27599.

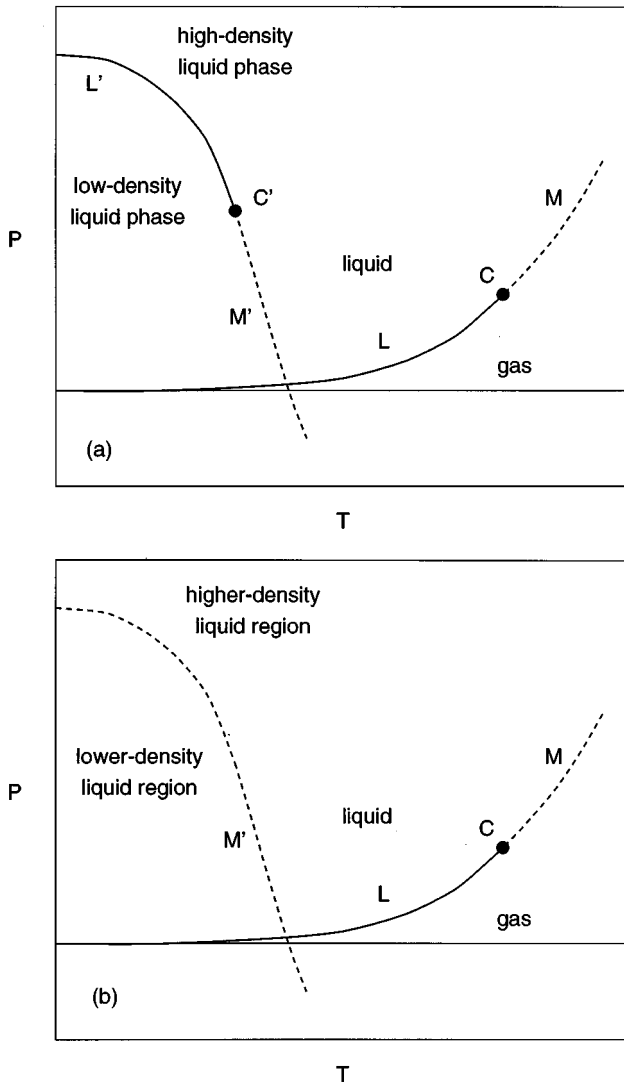


FIG. 1. (a) Schematic proposal for the  $P$ - $T$  phase diagram of liquid water. The line of first-order phase transitions  $L$  separates the liquid and gas phases and ends in the critical point  $C$ . The dashed line  $M$  is the line of  $K_T$  maxima observed in the supercritical region. At low  $T$  a line of first-order phase transitions  $L'$  separates distinct high- and low-density phases of the liquid. The line  $L'$  terminates in a critical point  $C'$ , from which extends another line of  $K_T$  maxima, denoted  $M'$ . (b) Schematic phase diagram of liquid water in the case that there exists a line of  $K_T$  maxima ( $M'$ ) that does not develop into a critical point and line of phase transitions as in (a). Although  $M'$  identifies the boundary between higher- and lower-density liquid regions, the properties of the liquid vary continuously along paths crossing  $M'$ .

mechanism by which the liquid phase might develop an instability leading to liquid-liquid phase separation. Then we present an analysis of molecular coordination and structure (Sec. IV) and of transport properties (Sec. V) for the simulated liquid in the vicinity of the line of  $K_T$  maxima. If a phase transition exists at lower  $T$ , these data suggest what the structure and relaxation behavior of the two distinct liquid phases might be. Finally, in Sec. VI, we enumerate several experimental results relevant to the possible existence of a line of  $K_T$  maxima in real water, perhaps followed at lower  $T$  by a critical point and line of first-order phase transitions.

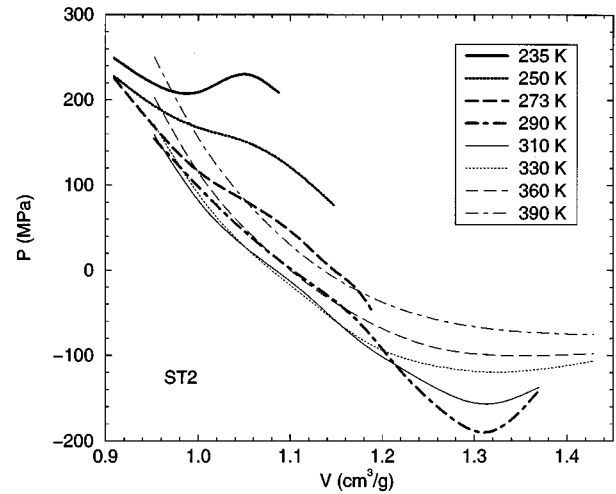


FIG. 2. Equation of state of liquid ST2. Plotted are isotherms of  $P$  versus  $V$  of a cubic spline through the data points tabulated in Ref. [20], from  $T=235$  K to  $T=390$  K.

## II. EQUATION OF STATE

Both the ST2 and TIP4P interaction potentials reproduce the thermodynamic anomalies of liquid water, including the density maximum, and the rapidly increasing  $K_T$  and  $C_P$  values in the supercooled region [26]. In order to determine the origin of these anomalies in the simulated liquid, we first examine the global behavior of the EOS. The EOS specifies how  $P$  depends on  $T$  and volume per unit mass  $V$ . In Fig. 2 we plot the EOS in terms of isotherms of  $P$  versus  $V$  for the ST2 interaction potential. The corresponding data for TIP4P are shown in Fig. 3 of Ref. [20].

At the highest  $T$ , the isotherms are decreasing functions of  $V$ , typical of simple liquid behavior. However, at lower  $T$ , the isotherms begin to develop a different shape, shown in Fig. 3(a). In particular, in the vicinity of  $V=1.1$  cm³/g, the sign of the curvature changes from positive to negative. The result is the appearance of a minimum in the slope of the isotherm. Moreover, the isotherm becomes progressively flatter as  $T$  decreases.

The isothermal compressibility  $K_T$  is related to the slope of a  $P$ - $V$  isotherm via

$$K_T \equiv -\frac{1}{V} \left( \frac{\partial V}{\partial P} \right)_T = \frac{1}{\rho} \left( \frac{\partial \rho}{\partial P} \right)_T, \quad (2.1)$$

where  $\rho \equiv 1/V$  is the density [27]. Evaluating  $K_T$  for ST2 from the  $P$ - $V$  isotherms in Fig. 3(a) yields a plot of  $K_T$  against  $V$  at constant  $T$ , shown in Fig. 3(b). In the vicinity of  $T=290$  K, a maximum appears in  $K_T$  and is observed at all lower  $T$  in the range in which we are able to conduct simulations. A similar analysis of the TIP4P  $P$ - $V$  data shows that this model also exhibits  $K_T$  maxima, which appear for  $T < 250$  K [Fig. 3(c)]. By finding the value of  $P$  corresponding to each of the maxima in Figs. 3(b) and 3(c), we locate the position in the  $P$ - $T$  plane of the line of  $K_T$  maxima (Fig. 4).

Since most experiments are conducted at constant  $P$  as opposed to constant  $T$ , we show in Fig. 5 plots of  $K_T$  for ST2 plotted along isobars rather than isotherms. The result shows

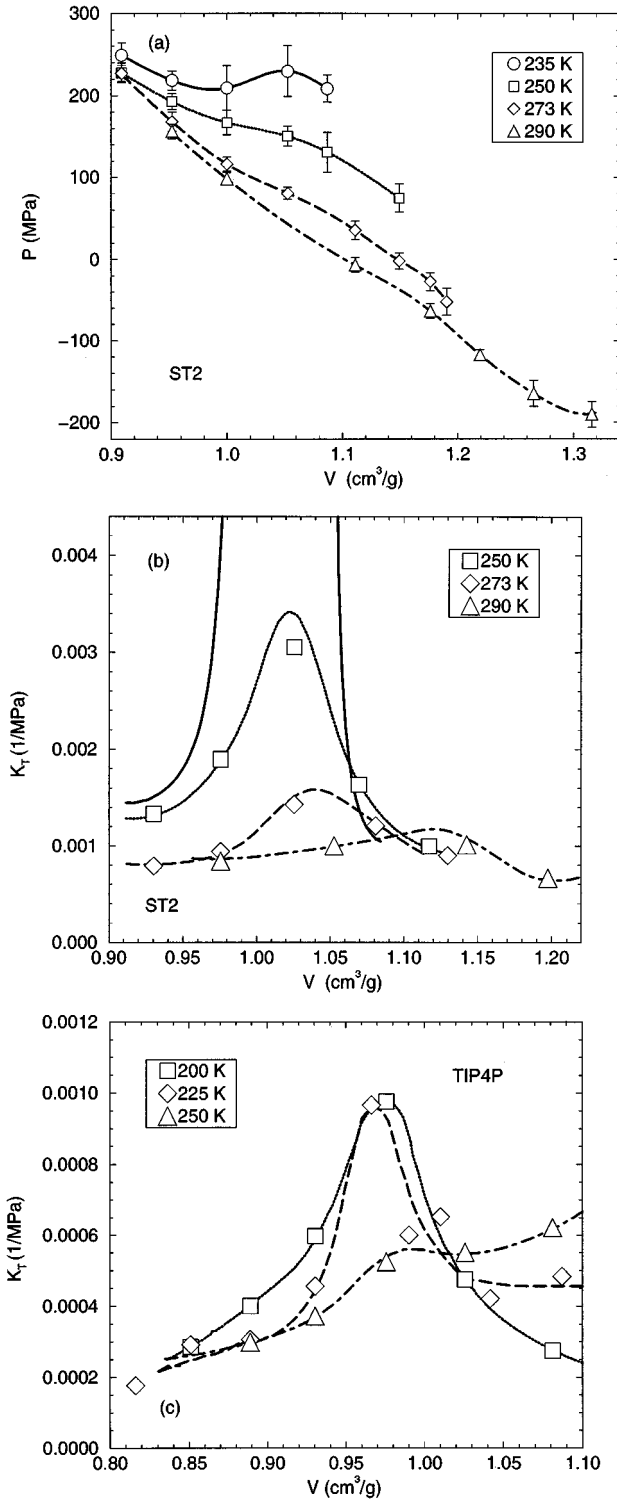


FIG. 3. (a) Isotherms of  $P$  versus  $V$  for ST2 at low  $T$ . The lines connecting the data points are the same splines shown in Fig. 2. (b) Isotherms of  $K_T$  versus  $V$  for ST2. Symbols represent  $K_T$  values calculated from the piecewise slope of the discrete data in (a). Curves give  $K_T$  as evaluated from the splines in (a), using Eq. (2.1), for  $T=290$  K (dot-dashed line),  $T=273$  K (dashed line),  $T=250$  K (dotted line), and  $T=235$  K (solid line). (c) Isotherms of  $K_T$  versus  $V$  for TIP4P. Symbols represent  $K_T$  values calculated from the piecewise slope of the discrete  $P$ - $V$  data tabulated in Ref. [20]. The lines are provided as guides to the eye. We do not analyze the TIP4P data via splines as in (a) and (b) because the relative error in the calculation of  $K_T$  for TIP4P is significantly larger than for ST2.

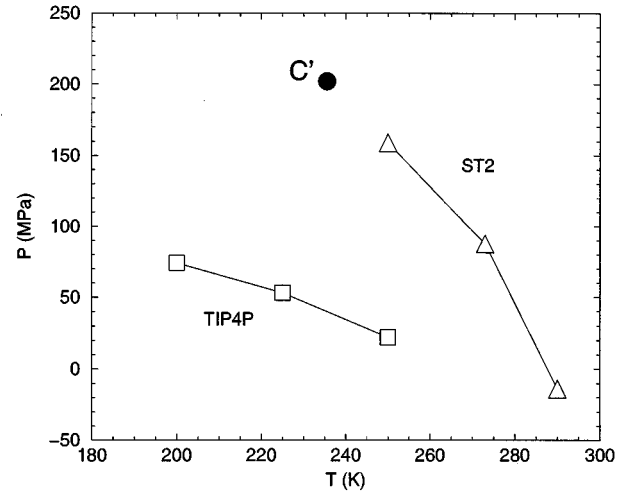


FIG. 4. Estimate of the position of the line of  $K_T$  maxima in ST2 ( $\Delta$ ) and TIP4P  $\square$ .  $C'$  labels the position of the critical point for ST2 as estimated from Fig. 6.

that the  $K_T$  maxima shown in Fig. 3(b) are also observed when the liquid is cooled along an isobar.

The occurrence of a line of  $K_T$  maxima in ST2 and TIP4P water is consistent with the prediction of Ref. [25]. Since the temperature of maximum density (TMD) line and the liquid-gas spinodal line do not intersect in these models,  $K_T$  must increase on cooling the system along an isobar below the TMD line. In real water, homogeneous nucleation of the crystal has so far prevented the experimental detection of either a divergence of  $K_T$  or the presence of a  $K_T$  maximum [3]. However, we show in Sec. VI that the existence of a maximum in  $K_T$  in the supercooled region of the phase diagram is consistent with the known behavior of water. Note also that lines of  $K_T$  maxima have been observed experimentally in other liquids, such as liquid Te [28], and have been found in computer simulations of liquid  $\text{SiO}_2$  [29].

In ST2 the magnitude of  $K_T$  at the maximum  $K_T^{\text{max}}$  increases as  $T$  decreases [Fig. 3(b)]. In Fig. 6(a) we plot

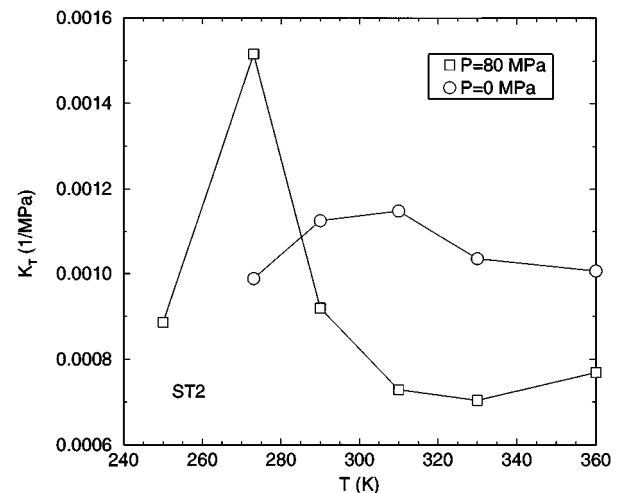


FIG. 5. Isobars of  $K_T$  as a function of  $T$  for  $P=0$  MPa ( $\circ$ ) and  $P=80$  MPa ( $\square$ ). To construct these isobars,  $K_T$  was evaluated for each  $T$  at the given  $P$  from the splines shown in Fig. 3(a).

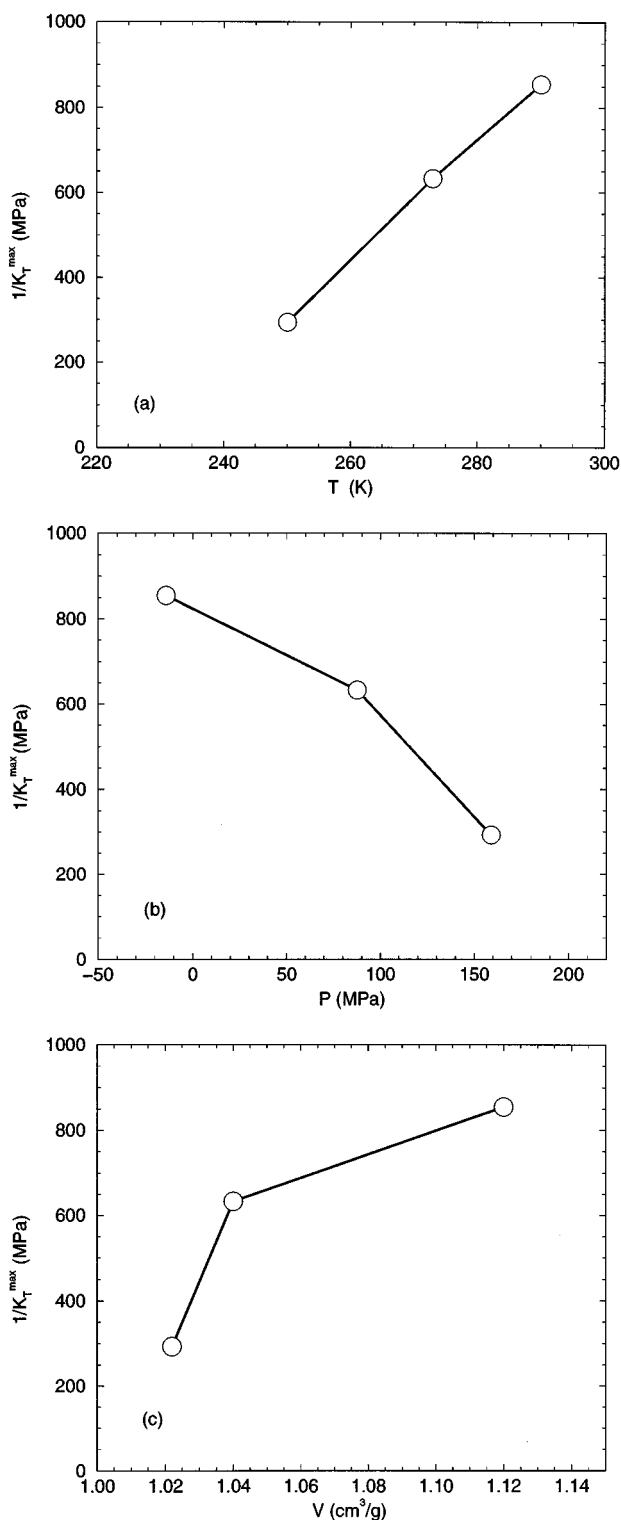


FIG. 6. Plots of  $1/K_T^{\max}$  for ST2 as a function of (a)  $T$ , (b)  $P$ , and (c)  $V$ . Extrapolation of each curve to zero yields an estimate of  $T_{C'}$ ,  $P_{C'}$ , and  $V_{C'}$ , respectively.

$1/K_T^{\max}$  as a function of  $T$ . If  $K_T^{\max}$  were to diverge, then  $1/K_T^{\max}$  would become zero. By extrapolating the data in Fig. 6(a), we find that  $1/K_T^{\max}$  appears to be approaching zero at a finite temperature  $T_{C'} \approx 235$  K. In Figs. 6(b) and 6(c) we show the corresponding plots of  $1/K_T^{\max}$  as a function of  $P$  and  $V$  respectively. Again, by extrapolation, we note that

$1/K_T^{\max}$  appears to approach zero at  $P_{C'} \approx 200$  MPa and  $V_{C'} \approx 1.02$   $\text{cm}^3/\text{g}$  (or  $\rho_{C'} \approx 0.98$   $\text{g}/\text{cm}^3$ ).

The divergence in  $K_T$  suggested by the ST2 data would indicate that a thermodynamic singularity appears on the line of  $K_T$  maxima at  $T_{C'}$ . In this case, the most likely behavior for  $T < T_{C'}$  would be that a line of first-order phase transitions extends from  $C'$  to lower  $T$ . In this scenario, the line of  $K_T$  maxima we observe is the supercritical precursor behavior expected above a critical point. For example, in the van der Waals description of a liquid-gas phase transition, the critical point is the terminus of a line of  $K_T$  maxima that occurs at higher  $T$  in the EOS of the supercritical fluid.

In the case that a critical point occurs, followed at lower  $T$  by a line of phase transitions, it is important to note that  $\rho$  (or equivalently  $V$ ) would be an appropriate order parameter. Hence, if the phase transition exists, it is a phase transition between two thermodynamically distinct liquid phases, identical in chemical composition, but differing in density, structure and transport properties [13]. Liquid-liquid phase transitions of this kind have been predicted theoretically [30–43] and via computer simulations [4,44,45] in several systems and have also been observed experimentally [46–49].

For TIP4P, we show the position of the line of  $K_T$  maxima in Fig. 4. The magnitude of these maxima is significantly smaller than for ST2 in the region of  $T$  accessible to simulation. Hence, with the present data we are unable to determine if the  $K_T$  maxima in TIP4P might develop into a divergence at lower  $T$ . From the location of the line of  $K_T$  maxima for TIP4P shown in Fig. 4 and from the EOS data of Ref. [20], we conclude that if a critical point  $C'$  occurs for TIP4P, it occurs at  $T < 200$  K and at  $P > 70$  MPa.

It was recently proposed [50] that TIP4P undergoes a first-order phase transition at  $T \approx 213$  K and  $P \approx 0.1$  MPa and that the critical point  $C'$  for TIP4P occurs at  $P < 0$ . This conclusion was based on results from simulations carried out in a constant- $P$  ensemble at several temperatures along isobars.

Our conclusion on the possible location of  $C'$  for TIP4P differs from that of Ref. [50]. To investigate the origins of this difference, we show in Fig. 7 both the EOS data for TIP4P presented in Ref. [20] and the corresponding data from Ref. [50]. We also show in Fig. 7 the density  $\rho$  and the configurational part of the internal energy  $U$  as functions of  $T$  taken from Refs. [20] and [50]. To compare data at the same state points, we use linear interpolation of the two closest thermodynamic states. As can be seen from Fig. 7, the results of Ref. [50] for the thermodynamic properties of TIP4P are in agreement (within the error bars) with those of Ref. [20]. Therefore, we conclude that the difference in the proposals regarding the location of  $C'$  for TIP4P is one of interpretation and is not due to differences in numerical results or simulation techniques.

The proposal of Ref. [50] that TIP4P exhibits a first-order phase transition at  $P \approx 0.1$  MPa and  $T \approx 213$  K was arrived at by interpreting the large changes in the values of the data points for  $\rho$  as a function of  $T$  along an isobar [Fig. 7(b)] as due to a jump discontinuity in the functional dependence of  $\rho$  around  $T = 213$  K. If this first-order transition occurs, then a van der Waals loop should occur in an isotherm of  $P$  ver-

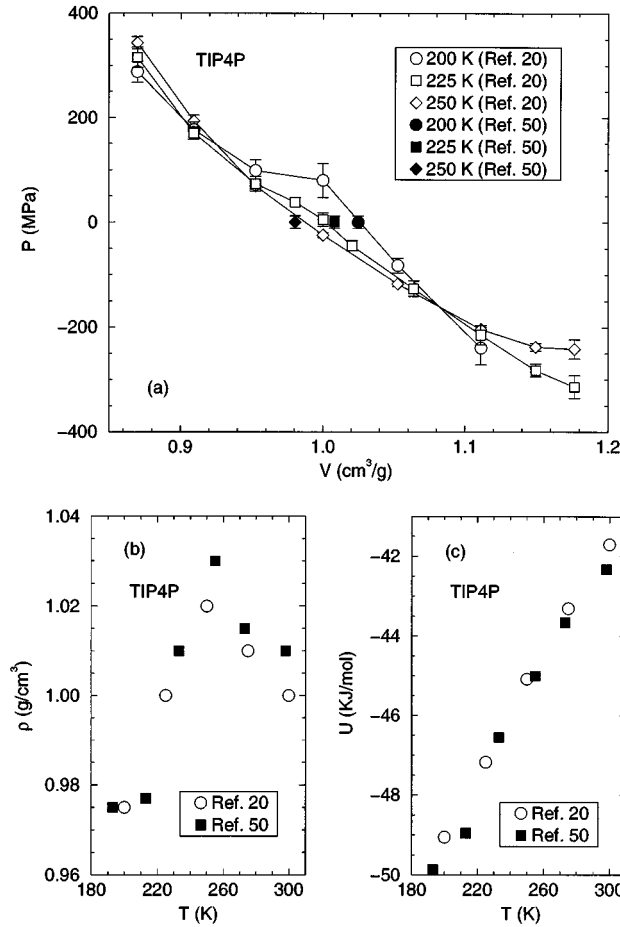


FIG. 7. Comparison of thermodynamic properties of TIP4P as evaluated in Refs. [20] and [50]: (a)  $P$ - $V$  isotherms, (b) isobar of  $\rho$  versus  $T$  at  $P=0.1$  MPa, and (c) isobar of  $U$  versus  $T$  at  $P=0.1$  MPa.

sus  $V$  at this  $T$  and also for  $T < 213$  K. The  $T=200$  K  $P$ - $V$  isotherm from Ref. [20] shown in Fig. 7(a) does not show such a van der Waals loop. Consequently we interpret the large changes in  $\rho$  versus  $T$  in Fig. 7(b) as continuous. That is, despite the large changes in thermodynamic properties found in *both* Refs. [20] and [50], the data shown in Fig. 7 do not support the occurrence of a discontinuous (i.e. first-order) transition for  $T > 200$  K. In this regard, further simulations are clearly required to determine more precisely the EOS for TIP4P over a wide range of  $P$  and  $T$ .

### III. INTERNAL ENERGY

Consider next the behavior of the configurational part of the internal energy  $U$ . In Fig. 8 we show isotherms of  $U$  as a function of  $V$  for the ST2 and TIP4P models [51]. At the higher  $T$  shown, an isotherm of  $U$  is a simple concave-upward (i.e., positively curved) function of  $V$ . However, as  $T$  decreases, a pronounced local minimum begins to appear. As we will show in the following sections, this state is characterized by a network of tetrahedrally coordinated water molecules and indicates the presence of an open molecular structure in the liquid that is particularly favorable energetically. The appearance of this minimum induces the curvature of the  $U$  versus  $V$  curve to become negative in the region

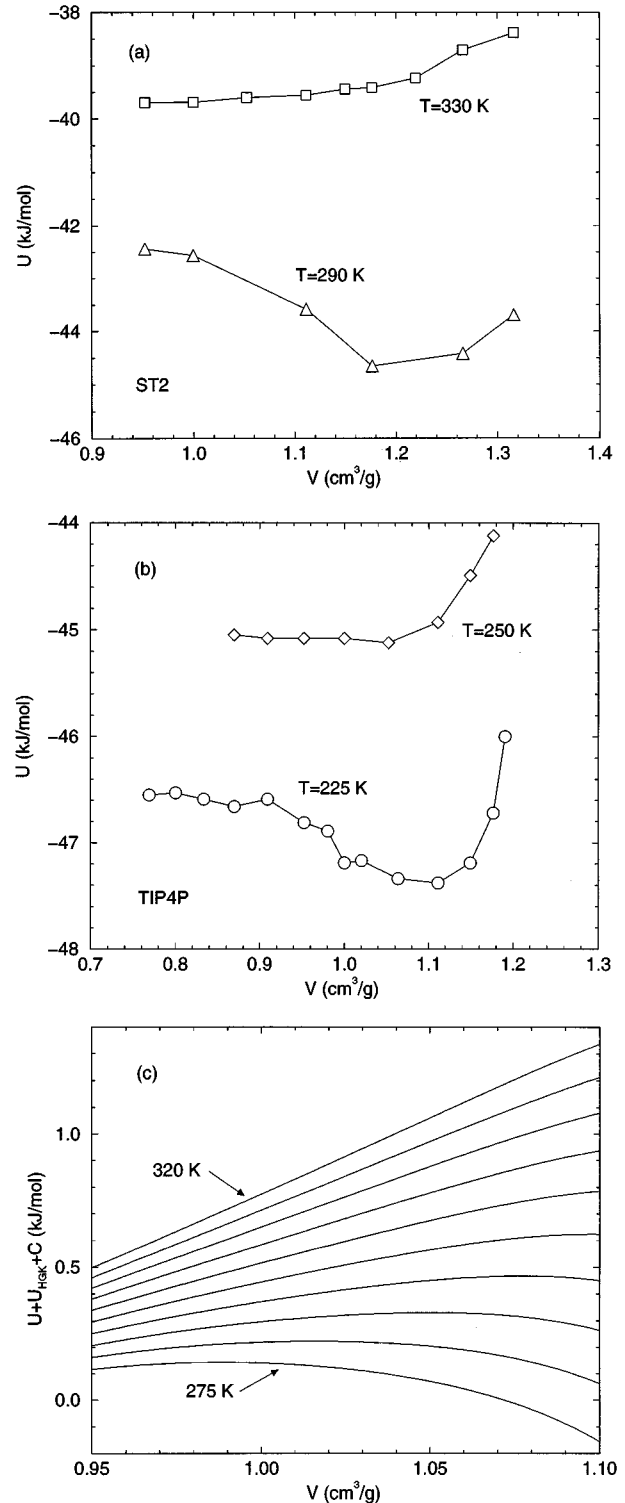


FIG. 8. (a) ST2 isotherms of  $U$  versus  $V$  at  $T=330$  K ( $\square$ ) and  $T=290$  K ( $\triangle$ ). (b) TIP4P isotherms of  $U$  versus  $V$  at  $T=250$  K ( $\diamond$ ) and  $T=225$  K ( $\circ$ ). (c) Isotherms of  $U$  as a function of  $V$  for real water, as evaluated from the Haar-Gallagher-Kell EOS [52]. The temperature is 275 K for the lowest curve and increases in steps of 5 K for each higher curve, up to  $T=320$  K for the top curve.  $U_{\text{HKG}}$  is a fixed parameter that normalizes the thermodynamic data to the properties at the triple point.  $C$  is an offset parameter to allow for convenient plotting of the data:  $C=0$  for the  $T=275$  K curve,  $C=-0.3$  kJ/mol for  $T=280$  K,  $C=-0.6$  kJ/mol for  $T=285$  K, and so on up to  $C=-2.7$  kJ/mol for  $T=320$  K.

below  $V = 1.15 \text{ cm}^3/\text{g}$  for ST2 and  $V = 1.05 \text{ cm}^3/\text{g}$  for TIP4P.

The Helmholtz free energy  $A$  is related to  $U$  via

$$A = U - TS, \quad (3.1)$$

where  $S$  is the entropy. The curvature of an isotherm of  $A$  must be positive for a homogeneous phase of a specified density to be thermodynamically stable [27]. From Eq. (3.1) the curvature of  $A$  can be expressed as

$$\left(\frac{\partial^2 A}{\partial V^2}\right)_T = \left(\frac{\partial^2 U}{\partial V^2}\right)_T - T \left(\frac{\partial^2 S}{\partial V^2}\right)_T. \quad (3.2)$$

Since

$$P = - \left(\frac{\partial A}{\partial V}\right)_T, \quad (3.3)$$

the inverse compressibility is related to the curvature of  $A$  [using Eq. (2.1)] by

$$\frac{1}{K_T} = V \left[ \left(\frac{\partial^2 U}{\partial V^2}\right)_T - T \left(\frac{\partial^2 S}{\partial V^2}\right)_T \right]. \quad (3.4)$$

Hence the curvature of  $A$  is proportional to  $1/K_T$  for fixed  $V$ ; that is,  $1/K_T$  must be positive for a thermodynamically stable state.

For the range of  $V$  in which  $(\partial^2 U/\partial V^2)_T < 0$ , the contribution of the internal energy is to *reduce*  $1/K_T$  and hence reduce the thermodynamic stability of the liquid phase. This is confirmed by the fact that the range of  $V$  in which we find negative curvature in the  $U$ - $V$  data corresponds to the range in which the  $K_T$  maxima are observed. The liquid remains stable where  $U$  has negative curvature only because the contribution of the entropic term in Eq. (3.2) is large enough to dominate. Yet entropic contributions to these thermodynamic quantities are suppressed as  $T$  decreases, due to the occurrence of the factor of  $T$  in the second term on the right-hand side of Eq. (3.2). Hence the  $U$ - $V$  data, like the  $P$ - $V$  data, suggest that at lower  $T$  a single homogeneous phase of the liquid will not be stable for certain values of  $V$ , leading to a separation into two distinct phases of higher and lower volume.

In Fig. 8(c) we show experimentally measured isotherms of  $U$  for real water plotted as a function of  $V$  for several temperatures, all greater than the freezing temperature [52,53]. These isotherms have small positive curvature at the highest  $T$  shown, but the curvature becomes negative as  $T$  decreases. Thus real water also exhibits the property that the behavior of the internal energy acts to *reduce* the stability of the liquid phase as  $T$  decreases.

## IV. STRUCTURAL PROPERTIES

### A. Coordination number

Next we examine the coordination number  $N_{NN}$  of the ST2 liquid as a function of  $T$  and  $V$ . Here  $N_{NN}$  is defined as the integral of the oxygen radial distribution function  $g_{OO}(r)$  from  $r=0$  to  $r=r_{\min}$ , where  $r_{\min}$  is the value of the interatomic distance  $r$  at which the first minimum appears in

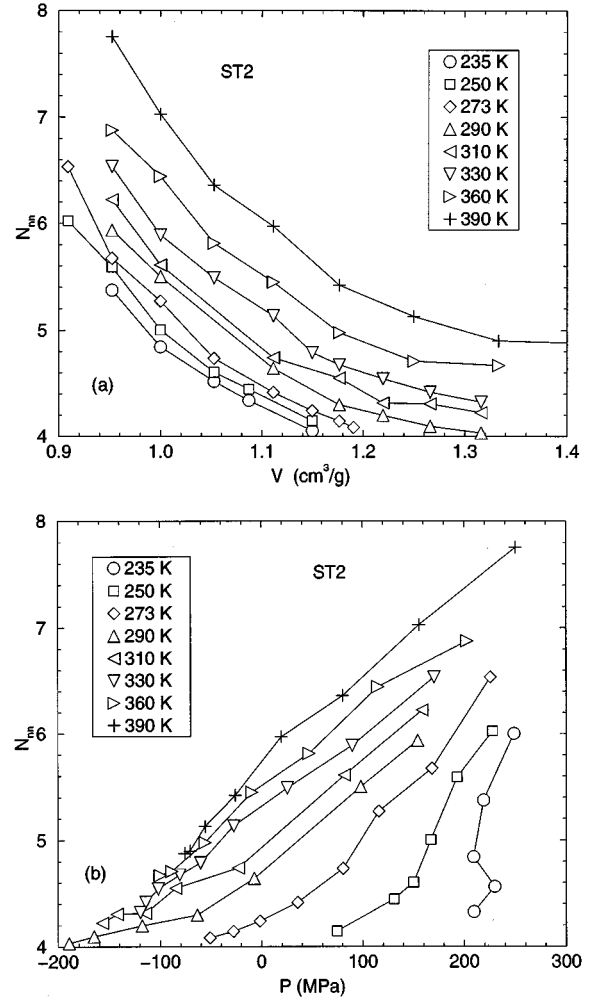


FIG. 9. (a) Isotherms of  $N_{NN}$  as a function of  $V$  for ST2 from  $T = 235 \text{ K}$  to  $T = 390 \text{ K}$ . (b) Isotherms of  $N_{NN}$  as a function of  $P$  for ST2 from  $T = 235 \text{ K}$  to  $T = 390 \text{ K}$ .

$g_{OO}(r)$ . Hence  $N_{NN}$  is the average number of nearest-neighbors found in the first coordination shell of an O atom.

Figure 9(a) shows isotherms of  $N_{NN}$  as functions of  $V$ . For  $T = 290 \text{ K}$  and below,  $N_{NN}$  decreases toward a limiting value of 4 as  $V$  increases.

We can also study the behavior of isotherms of  $N_{NN}$  as a function of  $P$  [Fig. 9(b)]. For the high- $T$  isotherms, the results show that a fourfold-coordinated configuration is approached at negative  $P$ , in agreement with previous simulations of Geiger and co-workers [54]. For  $T \leq 273 \text{ K}$ ,  $N_{NN}$  approaches 4 even for positive  $P$ , i.e., if  $P > 0$  and  $T$  is low enough, a fourfold-coordinated configuration can form [55].

The degree of abruptness with which  $N_{NN}$  decreases in Fig. 9(b) is also noteworthy. At high  $T$  the decrease of  $N_{NN}$  with  $P$  is smooth, but as  $T$  decreases,  $N_{NN}$  changes more abruptly from a structure with a large coordination number ( $N_{NN} > 6$ ) to a structure with  $N_{NN} \approx 4$ .

That a fourfold-coordinated network forms in liquid water is consistent with the possibility that a low-density liquid (LDL) phase can “condense” suddenly out of the high-density liquid (HDL) phase. The structure of the LDL phase resembles the structure of the random tetrahedral network (RTN) [56]. The RTN structure is usually thought of as ap-

pearing continuously as the liquid is cooled or stretched at low pressure. The present results show that a low-density, fourfold-coordinated structure occurs with increasing abruptness as  $P$  increases or  $T$  decreases.

Indeed, if a critical point  $C'$  were to exist, the two phases LDL and HDL are separated by a negatively sloped line of first-order phase transitions terminating at the point ( $T=T_{C'}$ ,  $P=P_{C'}$ ). If the system is cooled along an isotherm with  $P>P_{C'}$ , then as it crosses this first-order line the system will jump *discontinuously* from a HDL to a LDL phase, with a corresponding *discontinuous* density change. The extension of this first-order line into the one-phase region at larger  $T$  and lower  $P$  is the locus of  $K_T$  maxima, so when the system crosses this locus the system will change *continuously* from a liquid of higher local density ( $N_{NN}>4$ ) to a liquid of lower local density ( $N_{NN}\approx 4$ ). Thus our results suggest a relationship between the locus of  $K_T$  maxima and the changes in local structure as measured by the parameter  $N_{NN}$ .

### B. Radial distribution functions

The analysis of the preceding subsection indicates that a significant change occurs in the structure of the liquid when cooled through the region of the line of  $K_T$  maxima. In this section, we seek to characterize more precisely the structure of the liquid on either side of this line. For this purpose, we analyze the structure of the system in terms of the correlation function  $h(r)$ , defined as a weighted linear combination of the individual radial distribution functions:

$$h(r) = 4\pi\rho r [0.092g_{OO}(r) + 0.422g_{OH}(r) + 0.486g_{HH}(r) - 1]. \quad (4.1)$$

Here  $g_{OH}(r)$  and  $g_{HH}(r)$  are, respectively, the O-H and H-H radial distribution functions [57].

In particular, if there exists a critical point  $C'$ , then we would expect a two-phase coexistence region. To investigate the possible structural difference between these two phases, we study the structure of the liquid at a temperature close to the estimated value of  $T_{C'}$  at two values of  $\rho$  on either side of  $\rho_{C'}$ . This is equivalent to studying the structure of a liquid-gas system along a near-critical isotherm for densities smaller and larger than the liquid-gas critical density. In such a case the high-density structure would resemble the liquid structure, while the low-density structure would resemble the structure characteristic of the gas phase.

We calculate  $h(r)$  for ST2 at  $T=235$  K for  $\rho=1.05$  g/cm<sup>3</sup> (just above) and  $\rho=0.92$  g/cm<sup>3</sup> (just below) the estimated critical density  $\rho_{C'}=0.98$  g/cm<sup>3</sup>. Figure 10 shows the resulting  $h(r)$  functions, as well as the experimentally-measured  $h(r)$  for both the LDA and the HDA ice [55,58–61].

The structure of the liquid state of ST2 at  $\rho=1.05$  g/cm<sup>3</sup> is similar to the experimental data on HDA ice. We also find that the  $h(r)$  for LDA ice resembles our ST2 simulations of the liquid phase at  $\rho=0.92$  g/cm<sup>3</sup>. The correspondence between the HDA ice phase and ST2 water just above  $\rho_{C'}$  and between the LDA phase and ST2 water just below  $\rho_{C'}$  suggests that the two phases that become critical at  $C'$  in ST2

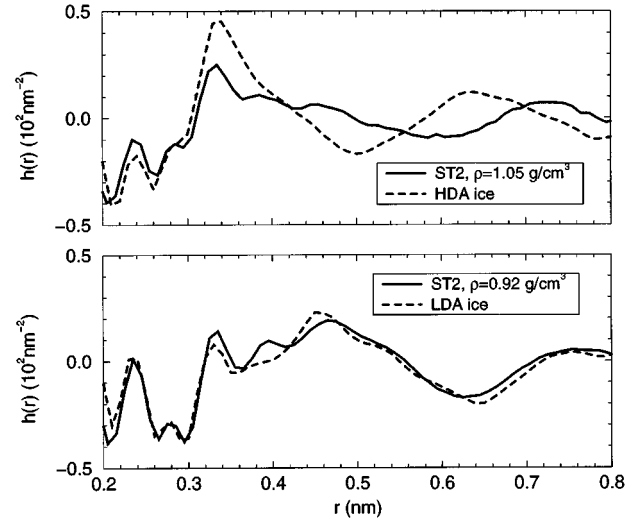


FIG. 10. Comparison of  $h(r)$  functions from experimental studies of HDA and LDA ice [55,58–61] (dashed lines) and from simulations of ST2 liquid (solid lines) at  $T=235$  K.

water are related to the known HDA and LDA phases of amorphous ice.

The possible existence of a critical point  $C'$  is supported by the fact that there is no broken symmetry between the structures of the LDA-like and HDA-like phases, as both phases are amorphous. If we assume that HDA and LDA ice are the glasses formed from the two liquid phases discussed above, then the HDA-LDA transition can be interpreted in terms of an abrupt change from one microstate in the phase space of the high-density liquid to a microstate in the phase space of the low-density liquid. The experimentally detected HDA-LDA transition line would then be the extension into the glassy regime of the line of first-order liquid-liquid phase transitions. Indeed, the original experimental studies of the HDA-LDA transition interpreted the observed behavior in terms of some kind of first-order transition [8].

The observed polyamorphism of amorphous ice is therefore consistent with, and supportive of, the possibility of a line of liquid-liquid phase transitions terminating in a critical point. However, polyamorphism in amorphous ice does not prove the existence of a phase transition in the behavior of the supercooled liquid. The possibility that there is no phase transition at any  $T$  can also account for abrupt density changes in the amorphous ices in the glass regime [13,25]. A line of  $K_T$  maxima extending to  $T=0$ , though not a line of phase transitions, nonetheless represents a line of states along which the glass will be highly compressible relative to nearby states points. A region of high but finite compressibility could have the same experimental effect on the behavior of the amorphous ices as a fully developed phase transition.

### V. TRANSPORT PROPERTIES

In this section we confirm the relationship between the behavior of  $N_{NN}$  for ST2 and the range of states where the molecular mobility begins to become too small for reliable simulations [54]. The molecular mobility, as quantified by the diffusion coefficient  $D$ , is shown from our ST2 simulations as a function of  $V$  in Fig. 11(a). The *decrease* in  $D$  as  $V$  increases at these values of  $T$  qualitatively reproduces the

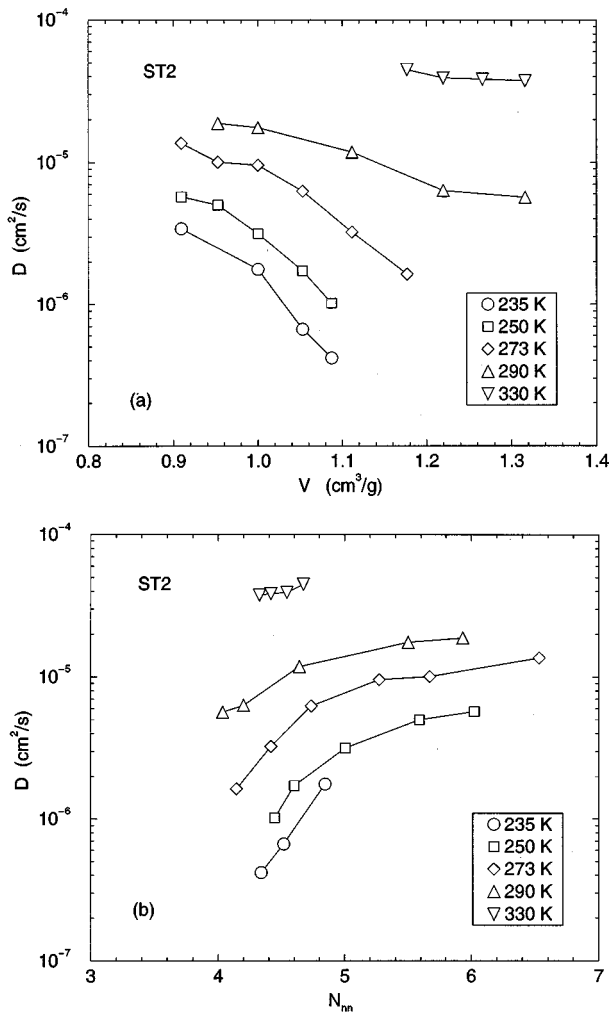


FIG. 11. Isotherms of  $D$  for ST2 as a function of (a)  $V$  and (b)  $N_{\text{NN}}$ .

dynamic anomaly observed in experimental measurements of  $D$  in supercooled water [62,63].

In Fig. 11(b), the information about  $D$  for ST2 is correlated with  $N_{\text{NN}}$  for the same states. There is a strong tendency for  $D$  to decrease rapidly as  $N_{\text{NN}} \rightarrow 4$  for the low-temperature isotherms. This observation confirms recent simulation work demonstrating the importance for molecular mobility of molecular environments having more than four nearest neighbors. It was found [64,65] that additional nearest neighbors beyond 4 have a ‘‘catalytic’’ effect on the mobility of the central molecule in that they lower the local energy barrier of the molecular exchanges that are the microscopic basis of diffusion. Consistent with this picture, Fig. 11(b) shows that  $D$  strongly decreases near  $N_{\text{NN}}=4$ . Therefore, Fig. 11(b) explains why we are unable to produce an equilibrated liquid, and evaluate the EOS, in ST2 simulations below a certain range of  $T$  and  $V$ : when the liquid approaches states with  $N_{\text{NN}}=4$ , the characteristic relaxation times of the liquid become very large [54,66–69]. Hence the low-density RTN form of the liquid that appears in supercooled water is intrinsically much more viscous than the liquid at higher  $T$  and so is difficult to study via simulation.

## VI. DISCUSSION

We have shown above that the EOS of both the ST2 and TIP4P models of water exhibit a line of  $K_T$  maxima. This confirms the prediction of Ref. [25] for liquids having a negatively sloped TMD line in the absence of a reentrant spinodal line. In addition, the results suggest that in the case of ST2, the line of  $K_T$  maxima develops into a critical point and line of liquid-liquid phase transitions. These results apply to the behavior of models of water. We now address the extent to which this behavior is consistent with the properties of real water as determined experimentally. In particular we should determine if the possibility of a line of  $K_T$  maxima, leading to a line of phase transitions, can be excluded as description of real water. In this regard we consider the following points.

(i) Though a line of  $K_T$  maxima has not been observed in real water, its existence cannot yet be excluded since nucleation of the ice phase inhibits the study of supercooled water [3]. If the phase behavior of Fig. 1 describes the properties of real water, then the observed behavior of  $K_T$  is due to the fact that presently we can only observe the approach one side of an as yet undetected  $K_T$  maximum.

(ii) Experimental measurements of the correlation length  $\xi$  of density fluctuations in supercooled water at atmospheric pressure do not show an increase in  $\xi$  as  $T$  decreases [70].  $\xi$  should increase close to a critical point and also on approach to the spinodal lines that connect to the critical point and lie on either side of a line of first-order phase transitions [71]. Hence, if they exist, the critical point and its associated spinodal lines must be located sufficiently far from the atmospheric pressure path followed in these experiments so as to be unaffected by critical fluctuations.

(iii) An appealing feature of the appearance of a critical point and line of phase transitions in supercooled water is the manner in which this proposal can rationalize and elucidate the rich behavior of liquid and amorphous solid water. To illustrate this, we present in Fig. 12 a schematic plot of the coexistence curves for the major phases of  $\text{H}_2\text{O}$  known experimentally, projected into the plane of  $T$  and  $\rho$  [1,72,73]. Also shown is the possible location of the metastable extension of the liquid side of the liquid-gas coexistence curve. The line  $L'$  in Fig. 12 represents the coexistence curve generated by the  $L'$  line shown in Fig. 1. Under  $L'$  the supercooled liquid is unstable as a single phase and will decompose into distinct high- and low-density liquids.

The existence of a region of unstable states for the supercooled liquid is perhaps not surprising, given the estimated positions of the stability fields of the crystal phases of ice. There is a relatively wide gap between the stability fields of ice I and ice II where no other crystalline form of ice is found [1]. This means that there are no stable local arrangements of molecules in this density range that are consistent with both thermodynamic stability as a single, homogeneous phase and long-range crystalline order. The fact that no stable crystalline structures are observed in this density range is consistent with the possibility that, at sufficiently low  $T$ , there are also no arrangements of molecules that are satisfactory for the appearance of a homogeneous liquid state.

(iv) The proposed location of the  $L'$  curve in Fig. 12



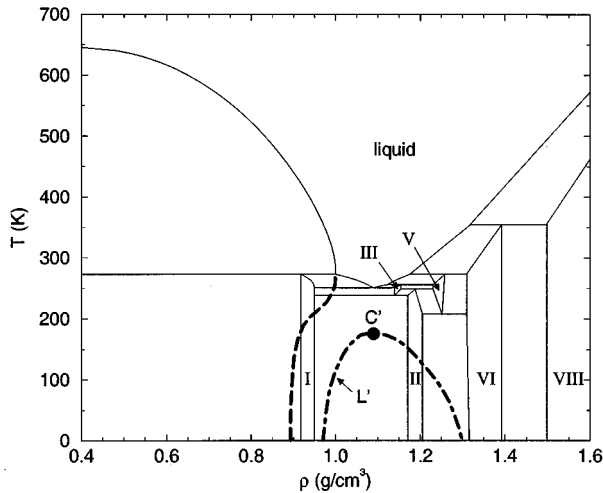


FIG. 12. Schematic plot of coexistence curves of liquid water and the major crystal polymorphs of  $\text{H}_2\text{O}$  (identified by roman numerals) [1,72,73]. The dashed line estimates the extension of the liquid side of the liquid-gas coexistence curve below the triple point.  $L'$  (dot-dashed line) estimates the coexistence curve that would appear in the supercooled region if a liquid-liquid phase transition occurred.

requires the liquid side of the liquid-gas coexistence curve to become a double-valued function of  $\rho$ . The liquid-gas coexistence curve reaches a maximum  $\rho$  and then retraces to lower  $\rho$  as  $T$  decreases. This behavior is required for the stability of the low-density liquid state at  $\rho \approx 0.92 \text{ g/cm}^3$ , a state that is not stable at ambient  $T$ . Though perhaps unexpected, this behavior of the liquid-gas coexistence curve is a known feature of the EOS of real water: the liquid-gas coexistence curve passes through a maximum  $\rho$  in the equilibrium regime, at a temperature just above the triple point [52].

(v) It is straightforward to understand how a density maximum appears in a liquid having a phase diagram of the form of Fig. 12. Consider an isobaric path starting from a high- $T$  state point at which  $\rho$  is less than that at the maximum in the liquid-gas coexistence curve. If this isobar does not pass into the unstable region inside the liquid-gas coexistence curve and if it terminates in the locally stable region near  $\rho = 0.92 \text{ g/cm}^3$  at low  $T$ , then it would necessarily have to pass through a maximum  $\rho$ .

(vi) As discussed above, the position of the line  $L'$  can simultaneously explain the thermodynamic anomalies of liquid water and the observed mechanical properties of the amorphous ices. Cooling the liquid brings the system closer and closer to the region of the critical point  $C'$  and its accompanying spinodal lines (not shown in Fig. 12). Hence there will be many paths along which thermodynamic response functions, such as  $K_T$  and  $C_p$ , will be observed to rise as  $T$  decreases. At the same time, the apparent mechanical instability of amorphous ice in the density range from  $1.0 \text{ g/cm}^3$  to  $1.25 \text{ g/cm}^3$  at much lower  $T$  is accounted for by the interval of unstable thermodynamic states lying under the coexistence curve  $L'$ .

(vii) The occurrence of liquid-liquid phase separation in deeply supercooled water would rationalize the success of so-called two-state models in describing water properties [38–43,74–80]. Models describing liquid-liquid phase separation

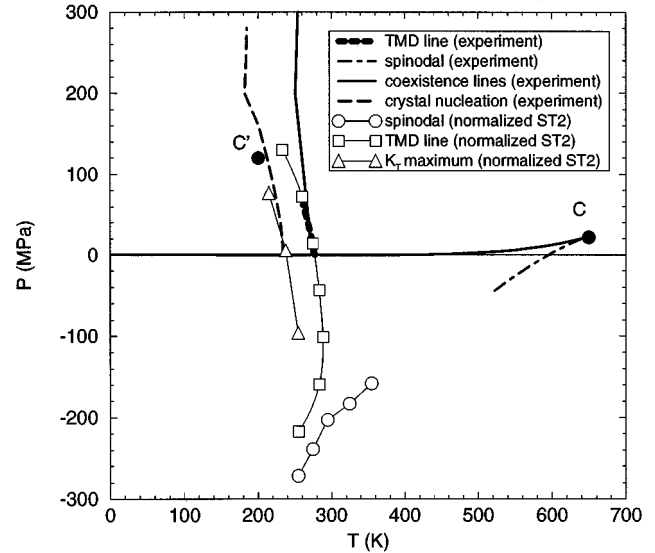


FIG. 13.  $P$ - $T$  phase diagram comparing experimentally known properties of water [3,52] with those determined from ST2 simulations. The positions of the ST2 data have been shifted by a constant amount ( $\Delta T = -35 \text{ K}$ ,  $\Delta P = -82 \text{ MPa}$ ) to bring the  $(P, T)$  location of the density maximum for  $V = 1.0 \text{ cm}^3/\text{g}$  into coincidence with the experimental position. The liquid-gas critical point is labeled  $C$ . The estimated position of the liquid-liquid critical point in ST2 is labeled  $C'$ .

in a one-component system have a formal relationship to the thermodynamics of a mixture [41,72,77]. If a liquid-liquid phase transition occurs in supercooled water, then the analysis of water properties in terms of a mixture—indeed, a highly nonideal mixture—is justified (for recent examples, see [79,80]).

(viii) In the absence of direct experimental data for the thermodynamic properties of water in the deeply supercooled region and for  $P \ll 0$ , we present in Fig. 13 a comparison of known water properties and those determined from ST2 simulations. To facilitate this comparison, we have shifted the ST2 properties in  $P$  and  $T$  [81] so as to bring the density maximum observed in ST2 into coincidence with that observed experimentally. With this adjustment, we see that the spinodal determined from ST2 simulations lies in an appropriate location at negative pressure to be consistent with the location of the spinodal near the liquid-gas critical point [52]. Also, we find that the line of  $K_T$  maxima approximately coincides with the observed homogeneous nucleation limit of crystalline ice [3]. If the liquid structure does indeed change rapidly toward the RTN structure as the line of  $K_T$  maxima is crossed, it would not be surprising to simultaneously observe a large increase in the crystal nucleation probability, since the local structure of the RTN and crystalline ice are quite similar.

## VII. CONCLUSION

We find that a line of  $K_T$  maxima occurs in the phase diagram of ST2 and TIP4P water. Moreover, in the case of ST2,  $K_T$  increases along this line as  $P$  increases and  $T$  decreases. This behavior suggests the possibility that the line of  $K_T$  maxima—the existence of which is demanded by the

behavior of the TMD and spinodal lines in these water models—develops at lower  $T$  into a thermodynamic instability. Though experimental confirmation of a line of  $K_T$  maxima in supercooled water does not yet exist, we find that the known properties of liquid and amorphous solid water are consistent with the behavior observed in simulation.

## ACKNOWLEDGMENTS

We would like to thank C.A. Angell, P.G. Debenedetti, T. Grande, P.F. McMillan, and S. Sastry for enlightening discussions. Financial support was provided by NSF and BP. P.H.P. acknowledges the support of NSERC (Canada).

- 
- [1] D. Eisenberg and W. Kauzmann, *The Structure and Properties of Water* (Oxford University Press, London, 1969).
- [2] For extensive information on the properties of water, see *Water: A Comprehensive Treatise*, edited by F. Franks (Plenum, New York, 1972).
- [3] C.A. Angell, *Annu. Rev. Phys. Chem.* **34**, 593 (1983).
- [4] W.D. Ludke and U. Landman, *Phys. Rev. B* **37**, 4656 (1988).
- [5] I. Ohmine and H. Tanaka, *Chem. Rev.* **93**, 2545 (1993).
- [6] R.J. Speedy and C.A. Angell, *J. Chem. Phys.* **65**, 851 (1976).
- [7] C.A. Angell, J. Shuppert, and J.C. Tucker, *J. Phys. Chem.* **77**, 3092 (1973).
- [8] O. Mishima, L.D. Calvert, and E. Whalley, *Nature (London)* **314**, 76 (1985).
- [9] O. Mishima, K. Takemura, and K. Aoki, *Science* **254**, 406 (1991).
- [10] O. Mishima, *J. Chem. Phys.* **100**, 5910 (1994).
- [11] G.H. Wolf, S. Wang, C.A. Herbst, D.J. Durben, W.J. Oliver, Z.C. Kang, and C. Halvorsen, in *High-Pressure Research: Application to Earth and Planetary Sciences*, edited by Y.S. Manghnani and M.H. Manghnani (American Geophysical Union, Washington, DC, 1992), p. 503.
- [12] C.A. Angell, P.H. Poole, and J. Shao, *Nuovo Cimento D* **16**, 993 (1994).
- [13] P.H. Poole, T. Grande, F. Sciortino, H.E. Stanley, and C.A. Angell, *Comput. Mater. Sci.* **4**, 373 (1995).
- [14] C.A. Angell, *Science* **267**, 1924 (1995).
- [15] R.J. Speedy, *J. Chem. Phys.* **86**, 982 (1982).
- [16] R.J. Speedy, *J. Chem. Phys.* **86**, 3002 (1982).
- [17] R.J. Speedy, *J. Phys. Chem.* **91**, 3354 (1987).
- [18] F.H. Stillinger and A. Rahman, *J. Chem. Phys.* **60**, 1545 (1974).
- [19] W.L. Jorgensen, J. Chandrasekhar, J. Madura, R.W. Impey, and M. Klein, *J. Chem. Phys.* **79**, 926 (1983).
- [20] P.H. Poole, F. Sciortino, U. Essmann, and H. E. Stanley, *Phys. Rev. E* **48**, 3799 (1993).
- [21] P.H. Poole, F. Sciortino, U. Essmann, and H. E. Stanley, *Nature (London)* **360**, 324 (1992).
- [22] P.H. Poole, U. Essmann, F. Sciortino, and H. E. Stanley, *Phys. Rev. E* **48**, 4605 (1993).
- [23] H.E. Stanley, C.A. Angell, U. Essmann, M. Hemmati, P.H. Poole, and F. Sciortino, *Physica A* **205**, 122 (1994).
- [24] F. Sciortino, U. Essmann, P.H. Poole, and H.E. Stanley, in *Physical Chemistry of Aqueous Systems*, edited by H.J. White, J.V. Senger, D.B. Neumann, and J.C. Bellows (Begell House, New York, 1995).
- [25] S. Sastry, P. Debenedetti, F. Sciortino, and H.E. Stanley, *Phys. Rev. E* **53**, 6144 (1996).
- [26] See Figs. 2 and 3 of Ref. [20] and Fig. 5 of Ref. [21].
- [27] H.E. Stanley, *Introduction to Phase Transitions and Critical Phenomena* (Oxford University Press, Oxford, 1971).
- [28] Y. Tsuchiya, *J. Phys. Condens. Matter* **3**, 3163 (1991).
- [29] P.H. Poole, M. Hemmati, and C.A. Angell (unpublished).
- [30] P.C. Hemmer and G. Stell, *Phys. Rev. Lett.* **24**, 1284 (1970).
- [31] G. Stell, and P.C. Hemmer, *J. Chem. Phys.* **56**, 4274 (1972).
- [32] J.M. Kincaid, G. Stell, and C.K. Hall, *J. Chem. Phys.* **65**, 2161 (1976).
- [33] J.M. Kincaid, G. Stell and E. Goldmark, *J. Chem. Phys.* **65**, 2172 (1976).
- [34] J.M. Kincaid and G. Stell, *J. Chem. Phys.* **67**, 420 (1977).
- [35] J.M. Kincaid and G. Stell, *Phys. Lett.* **65A**, 131 (1978).
- [36] A.C. Mitus, A.Z. Patashinskii, and B.I. Shumilo, *Phys. Lett.* **113A**, 41 (1985).
- [37] A.C. Mitus and A.Z. Patashinskii, *Acta Phys. Polon. A* **74**, 779 (1988).
- [38] E.G. Ponyatovsky and I.O. Barkalov, *Mater. Sci. Rep.* **8**, 147 (1992).
- [39] S. Sastry, F. Sciortino, and H.E. Stanley, *J. Chem. Phys.* **98**, 9863 (1993).
- [40] P.H. Poole, F. Sciortino, T. Grande, H.E. Stanley, and C.A. Angell, *Phys. Rev. Lett.* **73**, 1632 (1994).
- [41] E.G. Ponyatovsky, V.V. Sinard, and T.A. Pozdnyakova, *Pis'ma Zh. Éksp. Teor. Fiz.* **60** 352 (1994) [*JETP Lett.* **60**, 360 (1994)].
- [42] S.S. Borick, P.G. Debenedetti, and S. Sastry, *J. Phys. Chem.* **99**, 3781 (1995).
- [43] P.H. Poole, T. Grande, F. Sciortino, H.E. Stanley, and C.A. Angell (unpublished).
- [44] M. van Thiel and F.H. Ree, *Phys. Rev. B* **48**, 3591 (1993).
- [45] C.A. Angell, S. Borick, and M. Grabow (unpublished).
- [46] M.O. Thompson, G.J. Galvin, J.W. Mayer, P.S. Peercy, J.M. Poate, D.C. Jacobson, A.G. Cullis, and N.G. Chew, *Phys. Rev. Lett.* **52**, 2360 (1984).
- [47] E.P. Donovan, F. Saepen, D. Turnbull, J.M. Poate, and D.C. Jacobson, *J. Appl. Phys.* **57**, 1795 (1985).
- [48] S. Aasland and P.F. McMillan, *Nature* **369**, 633 (1994).
- [49] A. Ha, I. Cohen, X.-L. Zhao, M. Lee, and D. Kivelson, *J. Phys. Chem.* **100**, 1 (1996).
- [50] H. Tanaka, *Nature* **380**, 328 (1996); *J. Chem. Phys.* **105**, 5099 (1996).
- [51] See also Fig. 6 of Ref. [20].
- [52] L. Haar, J.S. Gallagher, and G. Kell, *NBS/NRC Steam Tables* (Hemisphere, Washington, DC, 1985).
- [53] These isotherms were generated using the computer program for generating EOS data provided in Ref. [52].
- [54] A. Geiger, P. Mausbach, and J. Schnitker, in *Water and Aqueous Solutions*, edited by G. W. Neilson and J. E. Enderby (Hilger, Bristol, 1986), p. 15.
- [55] This result is consistent with an experimental study of the evolution of the structure function  $S(q)$  as water is supercooled at atmospheric pressure, in which it was found that the structure

- tends toward that of the LDA ice (whose structure may resemble the LDL phase); see, e.g., M.-C. Bellissent-Funel and L. Bosio, *J. Chem. Phys.* **102**, 3727 (1995).
- [56] M.G. Sceats and S.A. Rice, in *Water: A Comprehensive Treatise*, (Ref. [2]), Vol. 7.
- [57] M. R. Chowdhury, J. C. Dore, and J.T. Wenzel, *J. Non-Cryst. Solids* **53**, 247 (1982).
- [58] A. Bizid, L. Bosio, A. Defrain, and M. Oumezzine, *J. Chem. Phys.* **87**, 2225 (1987).
- [59] M.-C. Bellissent-Funel, J. Teixeira, and L. Bosio, *J. Chem. Phys.* **87**, 2231 (1987).
- [60] M.-C. Bellissent-Funel, J. Teixeira, L. Bosio, and J.C. Dore, *J. Phys.: Condens. Matter* **1**, 7123 (1989).
- [61] M.-C. Bellissent-Funel, L. Bosio, A. Hallbrucker, E. Mayer, and R. Sridi-Dorbez, *J. Chem. Phys.* **97**, 1282 (1992).
- [62] E.W. Lang and H.-D. Lüdemann, *Angew. Chem. Int. Ed. Engl.* **21**, 315 (1982).
- [63] F.X. Prielmeier, E.W. Lang, R.J. Speedy, and H.-D. Lüdemann, *Phys. Rev. Lett.* **59**, 1128 (1987).
- [64] F. Sciortino, A. Geiger, and H.E. Stanley, *Nature (London)* **354**, 218 (1991).
- [65] F. Sciortino, A. Geiger, and H.E. Stanley, *J. Chem. Phys.* **96**, 3857 (1992).
- [66] C.A. Angell, *J. Phys. Chem.* **97**, 6339 (1993).
- [67] D. Paschek and A. Geiger (unpublished).
- [68] P. Gallo, F. Sciortino, P. Tartaglia, and S.-H. Chen, *Phys. Rev. Lett.* **76**, 2730 (1996).
- [69] F. Sciortino, P. Gallo, P. Tartaglia, and S.-H. Chen, *Phys. Rev. E* **54**, 6331 (1996).
- [70] Y. Xie, K.F. Ludwig, Jr., G. Morales, D.E. Hare, and C.M. Sorensen, *Phys. Rev. Lett.* **71**, 2050 (1993).
- [71] J.D. Gunton, M. San Miguel, and P.S. Sahni, in *Phase Transitions and Critical Phenomena*, edited by C. Domb and J.L. Lebowitz (Academic, London, 1983), p. 267.
- [72] T. Grande and P.H. Poole (unpublished).
- [73] Note that Fig. 12 is only qualitatively accurate. Though we have attempted to plot the data accurately where data exist, the locations of many of the coexistence lines shown are only partially known from experiments. This figure is presented as a thermodynamically self-consistent *possibility* for the overall phase diagram of H<sub>2</sub>O.
- [74] W.K. Röntgen, *Ann. Phys. (Leipzig)* **45**, 91 (1892).
- [75] H.S. Frank, in *Water: A Comprehensive Treatise* (Ref. [2]). Vol. 1.
- [76] H.E. Stanley and J. Teixeira, *J. Chem. Phys.* **73**, 3404 (1980); R.L. Blumberg, H.E. Stanley, A. Geiger, and P. Mausbach, *ibid.* **80**, 5230 (1984).
- [77] E. Rapoport, *J. Chem. Phys.* **46**, 2891 (1967).
- [78] C.A. Angell, *J. Phys. Chem.* **75**, 3698 (1971).
- [79] G.E. Walrafen and Y.C. Chu, *J. Phys. Chem.* **95**, 8909 (1991).
- [80] M. Vedamuthu, S. Singh, and G.W. Robinson, *J. Phys. Chem.* **98**, 2222 (1994).
- [81] Data in Fig. 13 are shown with a shift in  $T$  of  $-35$  K and a shift in  $P$  of  $-82$  MPa. The reasons for the shift are discussed in Ref. [21] and in F. Sciortino and S. Sastry, *J. Chem. Phys.* **100**, 3881 (1994).